Materials Letters 341 (2023) 134167

Contents lists available at ScienceDirect

Materials Letters

journal homepage: www.elsevier.com/locate/matlet

Study on the Structure *vs* Activity of Designed Non-Precious Metal electrocatalysts for CO_2 Conversion

Wangchao Yuan [a,1], Nivetha Jeyachandran [a,1], Tingke Rao [a], Azeem Ghulam Nabi [a,c], Matteo Bisetto [b], Devis Di Tommaso [a], Tiziano Montini [b], Cristina Giordano [a,*]

[a] Department of Chemistry, Queen Mary University of London, Mile End Road, London E14NS, UK
[b] Department of Chemical and Pharmaceutical Sciences, Center for Energy, Environment and Transport Giacomo Ciamician, INSTM Trieste Research Unit and ICCOM-CNR Trieste Research Unit, University of Trieste, Via Licio Giorgieri 1, 34127 Trieste, Italy
[c] Department of Physics, University of Gujrat, Gujrat, 50700, Pakistan

ARTICLE INFO

Keywords:
Bimetallic electrocatalysts
Copper-tin nanoparticles
Urea-glass-route
CO_2RR

ABSTRACT

This work investigates Cu and Cu-Sn nanocatalysts with controlled composition and morphology for the electrochemical CO_2 reduction reaction to value-added chemicals, showing that bimetallic materials possess active sites with increased specific activity toward activation and reduction of CO_2 compared to monometallic ones. While Cu showed high selectivity for the competitive hydrogen evolution reaction, bimetallic Cu-Sn electrocatalysts were selective towards CO and formates. Nanoparticles were prepared via a straightforward chemical process, leading to small, well-define and crystalline nanoparticles, either mono or bimetallic, where Cu and Sn precursors are blended in one step to achieve alloyed or core–shell structures.

1. Introduction

The electrochemical CO_2 reduction reaction (CO_2RR) has emerged as a promising strategy for converting CO_2 into value-added chemicals including methanol, methane, formic acid, formaldehyde, ethylene and ethanol [1]. The main challenges in CO_2RR lie in the activation of CO_2 while minimizing competitive pathways such as the production of hydrogen.

Copper (Cu) CO_2RR catalysts are the most promising for producing CO and other multi-carbon products [1] but lacks selectivity [2]. Strategies adopted to improve Cu performances include surface modification [3], metal doping [4] and alloying [5–8] to promote the adsorption/activation of CO_2 and improve stability, and nano-structuring [9] to expose a higher fraction of corner/edge surface atoms. These findings increased the interest in the tailored synthesis of Cu nanoparticles with fine control over crystallinity, size and porosity, to maximize catalytic activity, and tailor selectivity. The present contribution introduces an alternative green methodology, based on a sol–gel procedure called urea-glass-route [10], to prepare monometallic Cu and Sn, and bimetallic Cu-Sn nanoparticles. Compared to standard preparation methods, this route led to small, yet well-defined and crystalline nanoparticles with controlled composition and structure (from nano-alloy to core–-shell) in a straightforward way, without the use of any additive, support or co-catalyst. The as-prepared particles were tested for CO_2RR: while monometallic systems favour H_2 production, bimetallic electrocatalysts produce mainly CO and formates.

2. Result and discussion

Monometallic Cu(0) and Sn(0) nanoparticles were synthesized modifying the urea-glass-route [10], using different strategies to achieve CuSn alloy (*strategy A*) and either Cu@Sn (*strategy B*) or Sn@Cu (*strategy C*) core–shell nanoparticles (see SI).

Details on phases and structural properties of the synthesized samples were achieved by XRD study. Patterns were indexed and fitted by the Rietveld method. **Table SI.1** reports weight fractions, mean crystallite size and cell parameters of the phases identified in each sample. Fig. 1 shows the XRD patterns of CuSn samples prepared via the different strategies. For CuSn alloys, the XRD pattern (Fig. 1**A)** shows the formation of three phases identified as SnO_2, intermetallic Cu_3Sn and Cu (0). Here, Cu(0) peaks are slightly shifted (to lower angles) compared to those of monometallic Cu(0), somehow suggesting a (partial)

* Corresponding author.
E-mail address: c.giordano@qmul.ac.uk (C. Giordano).
[1] These authors contribute equally to the paper

https://doi.org/10.1016/j.matlet.2023.134167
Received 5 November 2022; Received in revised form 15 January 2023; Accepted 4 March 2023
Available online 8 March 2023

incorporation of Sn in the Cu structure. This finding seems plausible considering the similar atomic radii of the two metals: 128 pm and 140 pm for Cu and Sn, respectively. The formation of an alloyed Cu-Sn phase is also evident by the comparison with the pattern of the physical mixture (PM), which only shows two distinct phases: the expected patterns of pristine Cu(0) and Sn(0).

Cu@Sn-B XRD pattern shows the typical Cu(0) reflections, with asymmetric peaks and a visible shift towards lower angles (compared to monometallic Cu), suggesting again a structure expansion (confirmed by Rietveld analysis) due to intercalation of Sn atoms (Fig. 1**B**). Although the Cu@Sn pattern showed a Cu-rich phase, the presence of Sn closely connected to Cu was observed via elemental mapping (*vide infra*).

Finally, Sn@Cu-C XRD pattern (Fig. 1**C**) shows again the formation of Cu(0), Cu_3Sn, Sn and SnO_2 phases, and a slight shift toward lower angles of the Cu(0) phase, indicating again the close proximity of Sn to Cu.

XRD study highlighted that samples prepared with different strategies lead to different products, but in each case Cu is the leading phase, for the formation of a Cu(0) phase is always observed, albeit affected by the presence of Sn; conversely, Cu strongly affects the chemical behaviour of Sn. Increasing the initial amount of urea (from an urea/metal molar ratio R3 to R5) favors Cu-Sn interactions, as indicated by a higher content of the intermetallic Cu_3Sn phase. Surprisingly, no carbon phase (typical side product when urea is used) has been ever observed.

For information on large-scale morphology and general homogeneity, electron microscopy (transmission, TEM, and scanning, SEM) was used alongside elemental mapping analysis. **Figure SI.5** reports representative images of monometallic samples, showing that both Cu(0) and Sn(0) samples are composed by highly interconnected, polycrystalline and polydisperse particles, with size larger than the average crystalline size determined by XRD. Corresponding elemental mapping of monometallic Cu(0) showed the homogeneous presence of Cu (**Figure SI.6**), while the monometallic Sn(0) sample shows two phases (**Figure SI.7**), the second layered phase was identified as carbon. For the bimetallic phases (Fig. 2), CuSn alloy (*via* strategy A) shows a layered structure, very "bulky" and with no evident porosity. For Cu@Sn sample (*via* strategy B), clusters of elongated structure, polydisperse in size, are observed. In each case, elemental mapping has nicely shown that Cu and

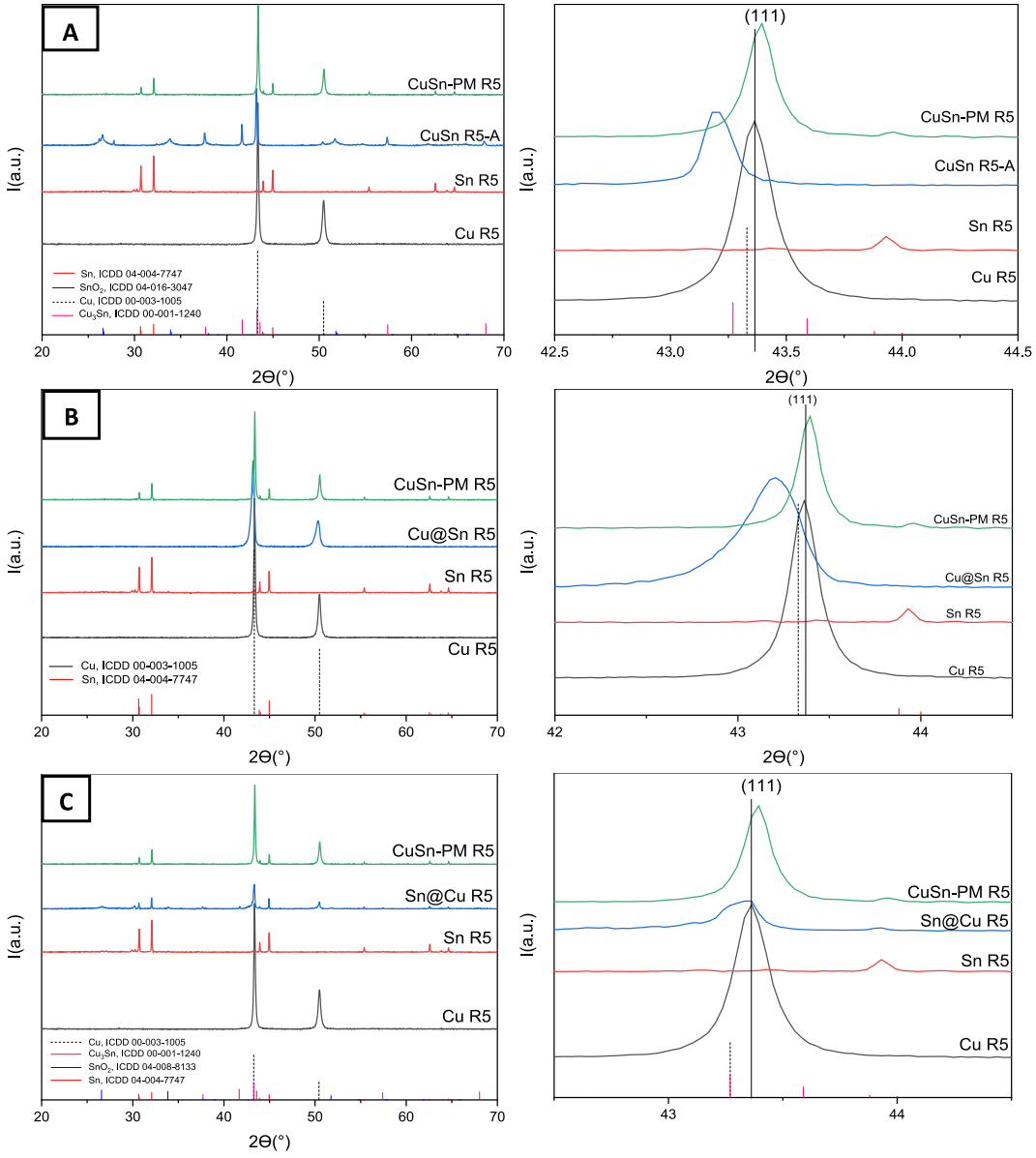

Fig. 1. XRD patterns of CuSn (1:1) samples prepared with different strategies (A, B, C). The ICDD patterns of pure Cu (ICDD 00–003-1005), Sn (ICDD 04–004-7747) and corresponding CuSn physical mixture (PM) are also reported for comparison. Right: magnified 42-44° range, around the Cu (1 1 1) peak.

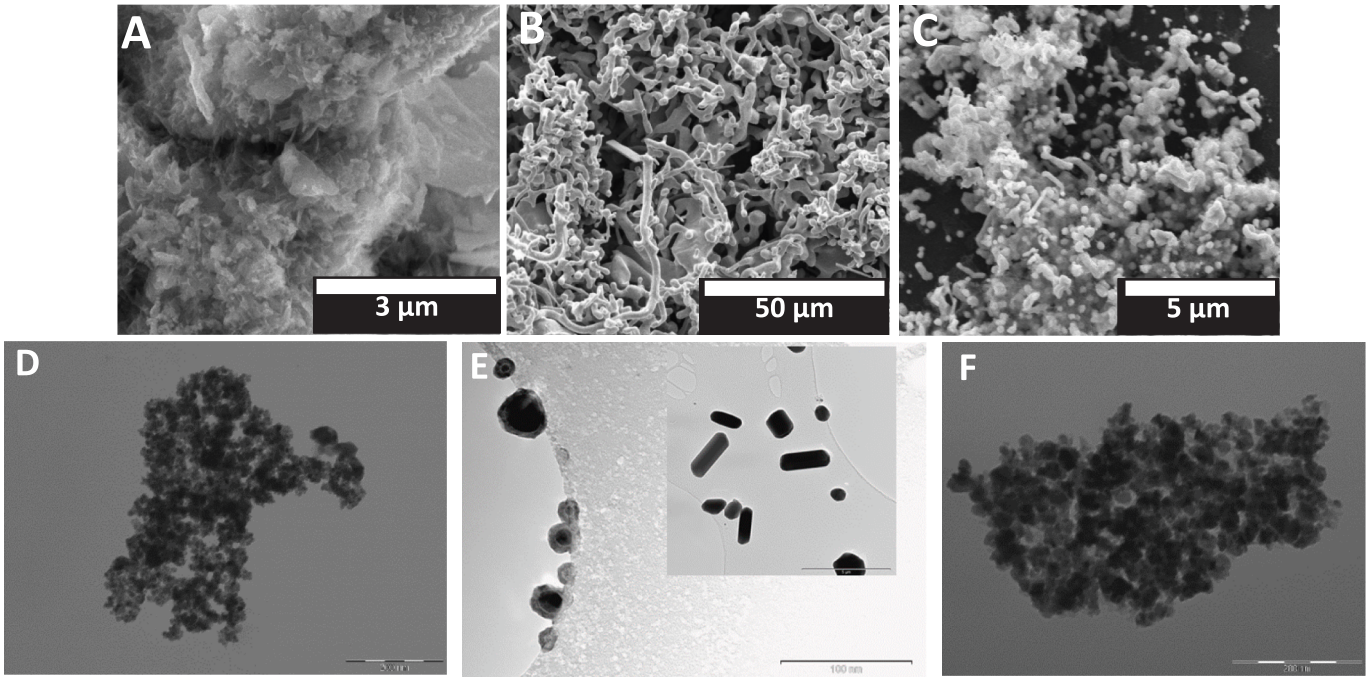

Fig. 2. Representative SEM and TEM images of CuSn R3 (A, D), Cu@Sn-B R5 (B,E) and Sn@Cu-C R5 (C, F).

Sn are in close contact (**Figure SI.9–13**). In some cases, the presence of oxygen is also observed but mainly onto the carbon phase. TEM investigation (Fig. 2), have shown, the formation of relatively small nanoparticles' clusters (in line with XRD results) but, more interesting, the formation of Cu@Sn core–shell nanoparticles. Although, at this magnification, TEM does not provide phase identification, the presence of the so-called "ghosts" around the particles (shining reflection) indicated the metallic nature of those phases. The occasional presence of a layered structure was also observed.

2.1. *Electrocatalytic CO_2 reduction reaction*

The role of alloying and morphology for bimetallic Cu-Sn was investigated toward the electrocatalytic CO_2RR. Cyclic Voltammetries (CVs) under CO_2 atmosphere reaching various negative potentials have shown similar trends (**Figure SI.19**): monometallic materials show higher current densities, indicating a higher tendency to exploit electrons for catalyzing electrocatalytic processes. Comparison of preliminary CVs and Chronoamperometries (CAs) under inert Ar or CO_2 (**Figure SI.20**) shows that very limited differences are observed for the monometallic Cu R3 samples, while for the bimetallic Cu@Sn-B and Sn@Cu-C, the current densities under CO_2 atmosphere are much higher than the case of Ar, suggesting a significant contribution from the CO_2RR process. A comparison of the materials' performances from this study and similar systems present in literature is reported in **Table SI.4**.

The performance of the materials towards CO_2RR was investigated in details by CA applying a constant potential for 1 h. As a representative example, the results obtained at – 1.5 V *vs* Ag/AgCl sat. are reported in Fig. 3, while the results obtained for other potentials (– 1.3 and –1.7 V *vs* Ag/AgCl sat.) are presented **Figure SI.21–22**. Similar trends have been obtained at different potentials, with the measured current densities and the production rates increasing as the potential becomes more negative. Notably, only at the most negative potential detectable amounts of ethylene have been observed. All the monometallic materials produce H_2 as main product, with Cu systems having higher current densities than Sn ones. All the monometallic materials had shown a faradaic efficiency towards H_2 (FE_{H2}) of around 60 – 70 % (Fig. 3**E**), indicating a higher selectivity in promoting H_2 production. Conversely, bimetallic materials show higher selectivity for production of carbon-based compounds from CO_2. Despite lower current densities (Fig. 3**B**), Cu@Sn-B and Sn@Cu-C show increased production and FEs toward formate and CO (Fig. 3**D–F**). A similar effect is observed for all the investigated potentials (Fig. 3, **SI.21–22**), with the selectivity for the products of CO_2RR increasing as the applied potential becomes more negative. It must be underlined that the overall FEs for some bimetallic materials (Sn@Cu and CuSn prepared with different urea:metal molar ratio, R) significantly differ from 100% because of parasitic or secondary reactions, probably related to reduction of SnO_x species.

The electrochemical tests results clearly indicate a higher selectivity of bimetallic materials toward CO_2RR process: compared to the results obtained from monometallic catalysts, bimetallic materials bear higher activity toward CO_2RR, strongly limiting the production of H_2. To rationalize the preference towards H_2 production or CO_2RR, we have calculated the adsorption process and the elementary steps for the concerted proton-electron transfer to convert CO_2 to formic acid and carbon monoxide and for the competitive H_2 production (see SI). On pure copper, H_2 has a weaker surface binding than COOH and CO, the first two intermediates of the CO_2RR, leading to easier desorption. The energetics of the reaction is modified on Cu-Sn, which promotes the formation of C1 and C2 products.

3. Conclusion

Copper, tin and copper-tin electrocatalysts for CO_2RR were prepared via a sol–gel based route, which allowed the preparation of small, yet well-defined and crystalline nanoparticles with controlled composition (namely mono or bimetallic) and different structure (from nano-alloy to core–shell) in a straightforward way, without the use of additives and support. Three strategies were explored to change the final structure of the catalyst. It was observed that the Cu(0) leading phase is affected by the presence of Sn; conversely, Cu strongly affects the behaviour of Sn. Cu-Sn electrocatalysts exhibited improved activity towards CO and formates formation, showing that bimetallic materials possess active sites with increased specific activity toward CO_2RR.

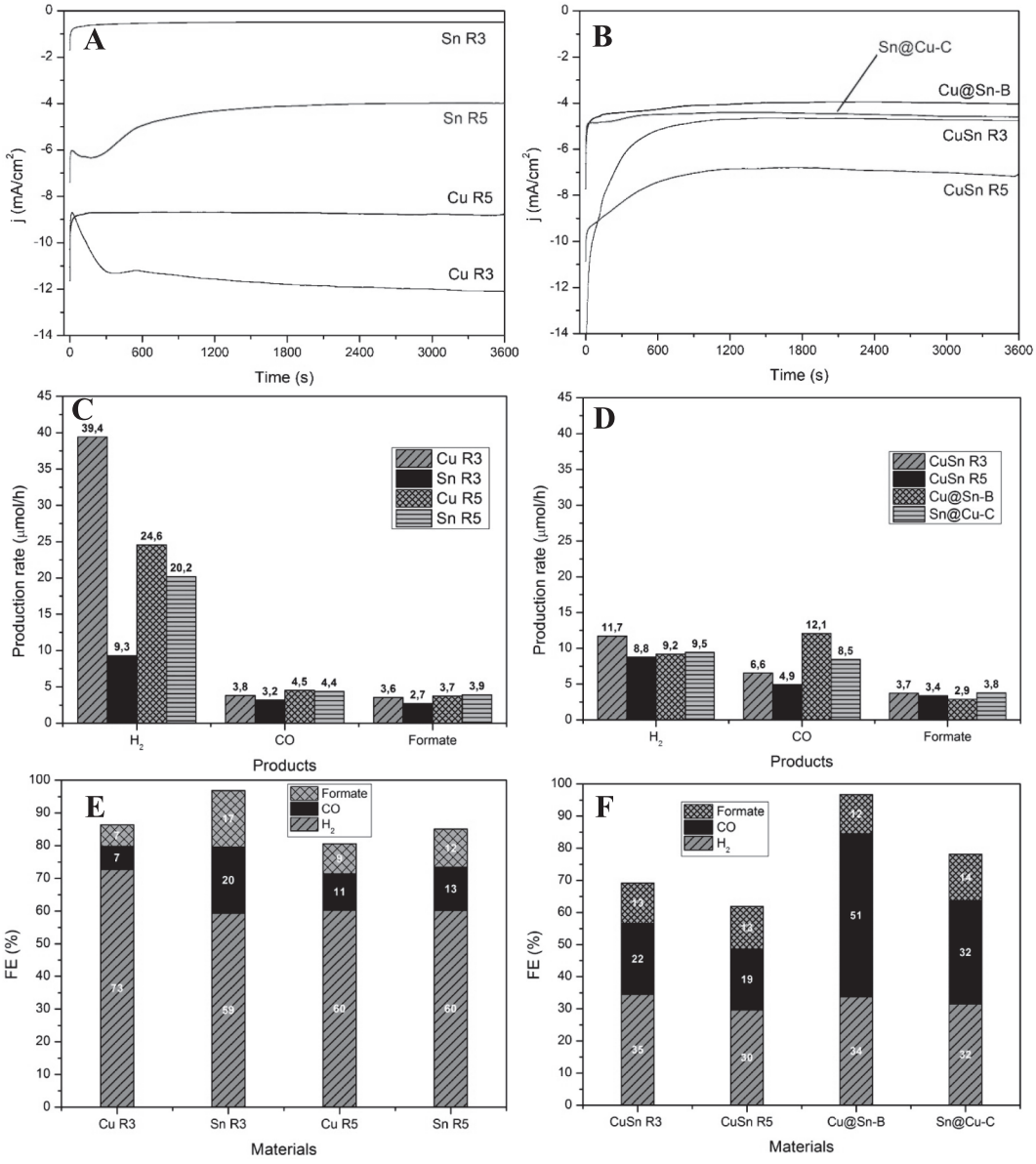

Fig. 3. Performance in electrocatalytic CO_2RR at the potential of – 1.5 V vs Ag/AgCl sat. of monometallic (left) and bimetallic (right) materials: (A, B) Chronoamperometries; (C, D) Production rate and (E, F) Faradaic Efficiencies (FE) for the detected products.

CRediT authorship contribution statement

Wangchao Yuan: Investigation, Validation, Data curation, Writing – original draft, Writing – review & editing. **Nivetha Jeyachandran:** Investigation, Validation, Data curation, Writing – original draft, Writing – review & editing. **Tingke Rao:** Investigation, Validation, Data curation, Writing – original draft, Writing – review & editing. **Azeem Ghulam Nabi:** Formal analysis, Data curation, Writing – original draft, Writing – review & editing. **Matteo Bisetto:** Investigation, Validation, Data curation, Writing – original draft, Writing – review & editing. **Devis Di Tommaso:** Conceptualization, Methodology, Resources, Supervision, Formal analysis, Data curation, Writing – original draft, Writing – review & editing. **Tiziano Montini:** Investigation, Validation, Data curation, Writing – original draft, Writing – review & editing. **Cristina Giordano:** Conceptualization, Methodology, Resources, Supervision, Investigation, Validation, Data curation, Writing – original draft, Writing – review & editing.

Declaration of Competing Interest

The authors declare that they have no known competing financial interests or personal relationships that could have appeared to influence the work reported in this paper.

Data availability

Data will be made available on request.

Acknowledgements

NJ acknowledges mini-Centre-for-Doctoral-Training in CO_2-Conversion@QMUL for PhD scholarship. W.Y&T.R. acknowledge the Chinese-Council-Scholarship for PhD scholarship. AGN acknowledges the Pakistan HEC-QMUL PhD Scholarships for funding. DDT acknowledged the ACT programme (Project No 299668), which funded the FUNMIN project. MB thanks University of Trieste for funding his PhD position. TM&MB acknowledge Prof. Paolo Fornasiero (Univesity of

Trieste) for helpful discussion and the financial support from University of Trieste (project FRA 2022), INSTM consortium and Italian Ministry of University and Research (project PRIN 2017PBXPN4).

Appendix A. Supplementary data

Supplementary data to this article can be found online at https://doi.org/10.1016/j.matlet.2023.134167.

References

[1] Y. Li, F. Cui, M.B. Ross, D. Kim, Y. Sun, P. Yang, Nano Lett. 17 (2017) 1312–1317.
[2] D.D. Zhu, J.L. Liu, S.Z. Qiao, Adv. Mater. 28 (2016) 3423–3452.
[3] S. Shen, J. He, X. Peng, W. Xi, L. Zhang, D. Xi, L. Wang, X. Liu, J. Luo, J. Mater. Chem. A 6 (2018) 18960–18966.
[4] J. Dean, Y. Yang, N. Austin, G. Veser, G. Mpourmpakis, ChemSusChem 11 (2018) 1169–1178.
[5] W. Xiong, J. Yang, L. Shuai, Y. Hou, M. Qiu, X. Li, M.K.H. Leung, ChemElectroChem 6 (2019) 5951–5957.
[6] S. Sarfraz, A.T. Garcia-Esparza, A. Jedidi, L. Cavallo, K. Takanabe, ACS Catal. 6 (2016) 2842–2851.
[7] X. Chen, D.A. Henckel, U.O. Nwabara, Y. Li, A.I. Frenkel, T.T. Fister, P.J.A. Kenis, A.A. Gewirth, ACS Catal. 10 (2020) 672–682.
[8] M. Morimoto, Y. Takatsuji, R. Yamasaki, H. Hashimoto, I. Nakata, T. Sakakura, T. Haruyama, Electrocatalysis 9 (2018) 323–332.
[9] B. Yang, C. Liu, A. Halder, E.C. Tyo, A.B.F. Martinson, S. Seifert, P. Zapol, L. A. Curtiss, S. Vajda, J. Phys. Chem. C 121 (2017) 10406–10412.
[10] C. Giordano, T. Corbiere, Colloid Polym. Sci. 291 (2013) 1297–1311.